8-Aza-2′-deoxyguanosine: Base pairing, mismatch discrimination and nucleobase anion fluorescence sensing in single-stranded and duplex DNA†

Frank Seela,* Dawei Jiang and Kuiying Xu

Received 23rd April 2009, Accepted 27th May 2009
First published as an Advance Article on the web 6th July 2009
DOI: 10.1039/b908017a

Oligodeoxyribonucleotides containing 8-aza-2′-deoxyguanosine **9** were synthesized and a new phosphoramidite **11**, showing a high coupling yield in solid-phase synthesis, was prepared. Nucleoside **9** was found to be a perfect shape mimic of dG; it forms a strong base pair with dC and shows an excellent mismatch discrimination. Nucleoside **9** appears strongly fluorescent as the anion, and thus, it has unique reporter group properties as a replacement for dG. The pK_a-value of **9** (8.4) is lower than that of dG (9.3) and increases from the single-stranded DNA (8.8) to duplex DNA (9.1). The fluorescence of the nucleoside **9** anion is decreased in ss-oligonucleotides and further reduced in duplex DNA. When mismatches of **9** are formed with the four DNA canonical bases, the fluorescence of mismatches is significantly higher than that of the perfectly paired duplex. The fluorescence of the nucleoside **9** anion correlates with the base pair stability.

Introduction

Canonical nucleobases of nucleic acids are practically non-fluorescent at room temperature; they show only significant emission in the frozen state or at extreme pH values.[1] In contrast, modified nucleosides of purin-2,6-diamine[2], purin-2-amine[2,3] or 2-oxopurine[4,5] (**1a–c**) (Scheme 1) as well as their pyrrolo[2,3-*d*]pyrimidine analogues (**2a–c**),[5–7] which can be considered as shape mimics of their parent purine nucleosides,[8] are fluorescent.‡ Related compounds such as the naturally occurring formycin (**3**)[2], ethenoA (**4a**) and its 2′-deoxy derivative (**4b**)[9,10], pyrroloC and its derivatives (**5a–d**)[11–13] and the thieno[3,4-*d*]pyrimidine nucleoside **6**[14] show also fluorescence. Guanosine develops fluorescence when the base is methylated at position-7 (**7**)[15] or an additional 5-membered ring is annelated, as in the tRNA constituent wyosine or its derivatives (**8a**,**b**).[16–19]

In contrast to the non-methylated guanosine, its derivatives 8-azaguanosine **9** and **10a**[21–23] (Scheme 2) are fluorescent in anionic form. Ribonucleoside **10a** shows a quantum yield of about 0.55 at pH 8.05,[20] and thus it can be used as a molecular reporter in nucleosides, nucleotides or oligonucleotides. As 8-azapurine nucleosides[24,25] have a similar shape to their canonical RNA or DNA constituents, their incorporation into DNA or RNA fragments is attractive. DNA and RNA fragments containing **9** and **10a** have already been synthesized enzymatically[20,21] or by solid-phase synthesis.[26,27] Also, the stability of duplexes containing **9** and the related 8-aza-2′-deoxyinosine (**10b**) has been studied.[26,28] This manuscript reports oligonucleotides with single or multiple incorporations of 8-aza-2′-deoxyguanosine (z^8G_d) **9**, and investigates the pH-dependent fluorescence, base pairing and the mismatch discrimination (T_m measurements) against the four canonical DNA constituents. For this purpose, the nucleobase of **9** was used in fluorescence sensing. A new phosphoramidite building block **11** is prepared that does not have the drawbacks of a previously reported compound[26] regarding protecting group stability and solubility.

Results and discussion

1. Synthesis and physical properties of 8-aza-2′-deoxyguanosine (9) and its phosphoramidite 11

The 8-azapurine base **12** has been synthesized but also occurs naturally, showing antifungal, antiviral and anticancer activity.[29–33] Mammalian and bacterial purine nucleoside phosphorylase (PNP) or *Bacillus cereus* cells accept 8-azaguanine as a substrate and convert it into the nucleoside if appropriate glycosyl donors are used.[20,34,35] Nucleobase-anion glycosylation was performed on azaguanine derivatives with 2-deoxy-3,5-di-*O*-*p*-toluoyl-α-D-*erythro*-pentofuranosyl chloride **13**[29] or with a 2,3-dideoxy-D-*glycero*-pentofuranosyl chloride.[36] By this route, 8-aza-2′-deoxyguanosine **9** as well as regioisomeric analogues were prepared under kinetically controlled conditions.[27] The reaction results in an inversion of the anomeric configuration with exclusive formation of β-D anomeric nucleosides. In another approach Robins *et al.*[37] used the fusion reaction employing the silylated 8-azaguanine **12** with the halogenose **13** (Scheme 3). The elevated temperature results in an equilibration of the halogenose **13** and yields an anomeric mixture of α-D and β-D isomers (**14** and **15**). No regioisomeric nucleosides were detected due to thermodynamic control of the reaction. Repeated crystallization in ethyl acetate yielded the pure β-D-anomer **15**. This synthetic route was used for the preparation of **9** and the DNA building block synthesis. For this purpose, the reaction protocol was slightly improved and nucleoside **9**

Laboratory of Bioorganic Chemistry and Chemical Biology, Center for Nanotechnology, Heisenbergstraße 11, 48149 Münster, Germany and Laboratorium für Organische und Bioorganische Chemie, Institut für Chemie, Universität Osnabrück, Barbarastraße 7, 49069, Osnabrück, Germany. E-mail: Frank.Seela@uni-osnabrueck.de, Seela@uni-muenster.de; Fax: +49 (0) 251 53 406 857; Tel: +49 (0)251 53 406 500; Web: www.seela.net

† Electronic supplementary information (ESI) available: ^{1}H and ^{13}C NMR spectra. See DOI: 10.1039/b908017a

‡ Purine numbering is used throughout the Results and discussion section of this article.

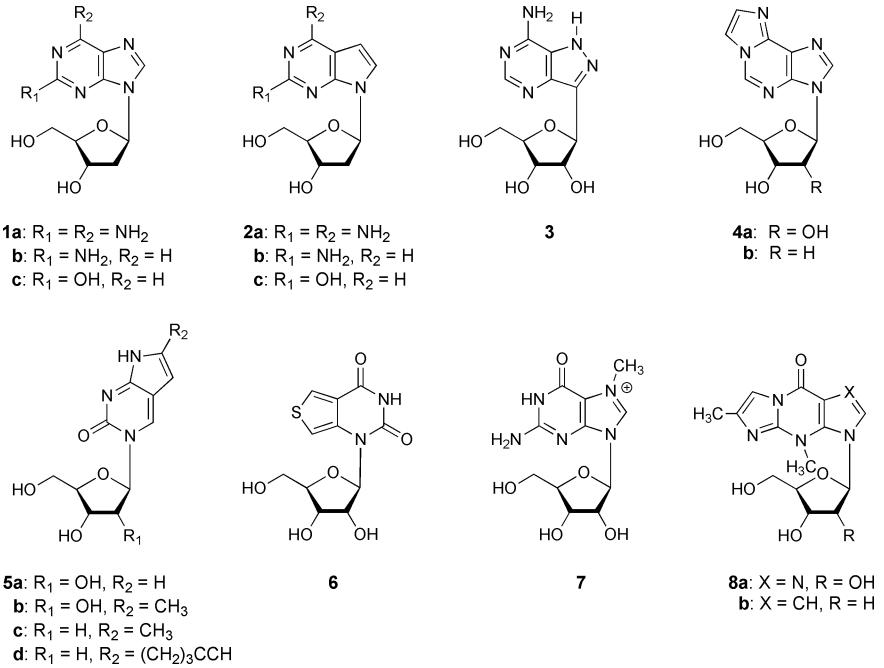

Scheme 1

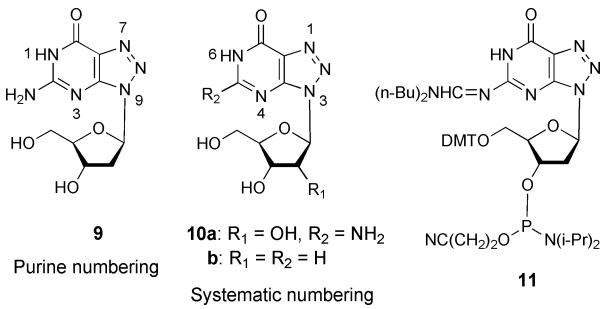

Scheme 2

and its derivatives were characterized in detail (NMR, UV). The amino group of **9** was protected with *N*,*N*-di-n-butylformamide dimethyl acetal[38] yielding derivative **16** (Scheme 3). Subsequently, compound **16** was converted to the 5′-*O*-dMT derivative **17** under standard conditions. Phosphitylation with 2-cyanoethyl-*N*,*N*-diisopropylphosphoramido chloridite furnished the phosphoramidite **11** (Scheme 3).

Table 1 provides a compilation of the ^{13}C NMR data of the 8-aza-2′-deoxyguanosine **9** and its derivatives. The assignment of ^{13}C NMR chemical shifts of the sugar moiety and the protecting groups was made on the basis of gated-decoupled spectra in combination with already published data.[26,27,36,39] The large coupling constant of 165 Hz of C-1′[40] compared to those of

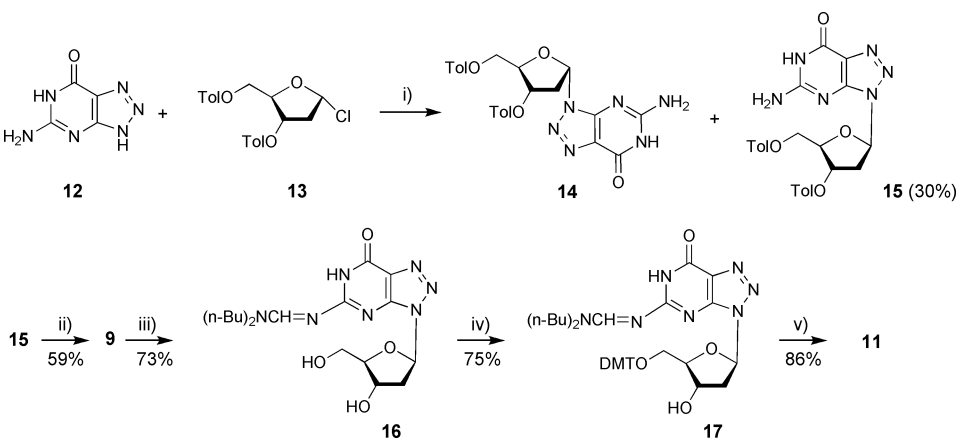

Scheme 3 *Reagents and conditions:* i) Hexamethyl disilazane, reflux; fusion of the silyl derivative with halogenose **13** at 130 °C under reduced pressure. Recrystallization of the **14**/**15** mixture from EtOAc gave **15**.[37] ii) NH_3/MeOH, 60 °C, autoclave. iii) *N*,*N*-dibutylformamide dimethyl acetal, MeOH, room temperature. iv) 4,4′-dimethoxyltriphenylmethyl chloride, pyridine, room temperature. v) 2-cyanoethyl-*N*,*N*-diisopropylphosphoramido chloridite, *N*,*N*-diisopropylethylamine, CH_2Cl_2, room temperature.

Table 1 ^{13}C NMR chemical shifts of 8-aza-2′-deoxyguanosine and related nucleosides. The assignments in the first four columns are tentative.[a]

	C(7)[b]	C(5)[b]	C(3a)[b]	C(7a)[b]									
	C(6)[c]	C(2)[c]	C(4)[c]	C(5)[c]	C(1′)	C(2′)	C(3′)	C(4′)	C(5′)	CH_3	CH_2	CH	$(MeO)_2Tr$
9	155.7	155.7	151.5	124.5	83.9	37.9	70.8	88.2	62.2	—	—	—	—
12[29]	156.3	155.1	153.8	123.8	—	—	—	—	—	—	—	—	—
15	155.7	155.5	151.6	124.5	84.0	35.2	74.7	81.9	63.9	—	—	—	—
16	160.0	158.6	150.4	126.6	84.3	38.1	70.8	88.2	62.1	13.5 13.7	19.1; 19.6 28.4; 30.3 45.3; 51.4	156.4	—
17	160.0	158.5	150.3	127.6	83.9	38.4	70.5	85.9	64.1	13.6 13.7	19.1; 19.6 28.5; 30.3 45.1; 51.4	156.5	54.9; 55.0

[a] Measured in DMSO-d_6 at 298 K. [b] Purine numbering. [c] Systematic numbering.

the other sugar carbons (about 150 Hz) was used to identify the anomeric ^{13}C NMR signal.

2. Oligonucleotide synthesis, characterization and hybridization

Next, the phosphoramidite **11** was employed in solid-phase oligonucleotide synthesis. Oligonucleotides were prepared as described in the experimental section and were purified by reversed-phase HPLC and characterized by MALDI-TOF spectra. The composition of oligomers was determined by enzymatic analysis[41] using snake-venom phosphodiesterase followed by alkaline phosphatase. The mixture was analyzed on reversed-phase HPLC (RP-18). Fig. 1a shows the HPLC profile of the enzymatic digest. For peak identification nucleoside **9** was added (Fig. 1b).

To investigate the influence of the base-modified nucleoside **9** on duplex stability and mismatch discrimination, the duplex 5′-d(TAGGTCAATACT) (**18**) · 3′-d(ATCCAGTTATGA) (**19**) was used as reference and was modified. The modified duplexes contain one or two incorporations of the base-modified **9** at various positions (Table 2). All duplex T_m values shown in Table 2 were measured in 1.0 M NaCl, 0.1 M $MgCl_2$, 60 mM Na-cacodylate at pH 7 or pH 8, and the thermodynamic data of duplex formation were calculated from each individual melting profile. The replacement of one or two dG-residues by 8-aza-2′-deoxy-guanosine **9** (T_m = 52 °C for **18**·**21** and T_m = 53 °C for **18**·**20**) has a positive effect on duplex stability.[26] As a shape mimic of dG, 8-aza-2′-deoxyguanosine **9** forms a strong base pair with dC which is slightly more stable than that of a dG·dC pair (Scheme 4). In order to evaluate mismatch discrimination,[42] the four canonical nucleosides were placed opposite to the modification site (duplexes 5′-d(TAGGT**X**AATACT) · 3′-d(ATCCA**9**TTATGA), X = dA, dG, dT, dC) and the T_m values were measured. The base discrimination of **9** against the four canonical DNA bases measured at pH 7.0 was found to be similar to that of dG. The T_m values of duplexes with mismatched base pairs are significantly lower ($\Delta T_m \approx -20$ °C) than that of the duplex **18**·**21** containing **9**·dC. A higher T_m value for the mismatch of **9** or dG with dT is observed in both series, most likely due to dG·dT or **9**·dT base pair formation (Scheme 4). Due to the lower pK_a value of **9**, the T_m value of the modified duplex **18**·**21** containing **9**·dC decreases more at higher pH values (9.3) than the unmodified duplex **18**·**19** and the mismatched duplexes (Table 3). All T_m measurements of Table 3 were performed in the absence of Mg^{2+} ions as the hydroxide precipitates at pH 9.3. Altogether, duplex stability decreases in the order dC·**9** ≫ dT·**9** > dA·**9** > dG·**9** within each series of T_m measurements (pH 7.0, 8.0, 8.4, 9.3).

Table 2 T_m values of oligonucleotide duplexes containing 8-aza-2′-deoxyguanosine **9** in a match and mismatch situation at pH 7.0 and 8.0.[a] Data for dG are given for comparison.[43]

Duplex		pH	T_m [°C]	ΔT_m [°C][b]	ΔG_{310} [kcal mol^{-1}][c]
5′-d(TAGGTCAATACT)	**18**	7	50	0	−11.8
3′-d(ATCCAGTTATGA)	**19**				
5′-d(TAGGT**C**AATA**C**T)	**18**	7	53	+3	−12.0
3′-d(ATCCA**9**TTAT**9**A)	**20**				
5′-d(TAGGT**C**AATACT)	**18**	7	52	+2	−11.9
3′-d(ATCCA**9**TTATGA)	**21**				
5′-d(TAGGT**G**AATACT)	**22**	7	30	−20	−6.6
3′-d(ATCCA**9**TTATGA)	**21**				
5′-d(TAGGT**T**AATACT)	**23**	7	35	−15	−7.3
3′-d(ATCCA**9**TTATGA)	**21**				
5′-d(TAGGT**A**AATACT)	**24**	7	33	−17	−6.9
3′-d(ATCCA**9**TTATGA)	**21**				
5′-d(TAGGT**C**AATACT)	**18**	8	50	0	−11.8
3′-d(ATCCA**G**TTATGA)	**19**				
5′-d(TAGGT**C**AATACT)	**18**	8	50	0	−11.8
3′-d(ATCCA**9**TTATGA)	**21**				
5′-d(TAGGT**G**AATACT)	**22**	8	30	−20	−6.5
3′-d(ATCCA**9**TTATGA)	**21**				
5′-d(TAGGT**T**AATACT)	**23**	8	34	−16	−6.7
3′-d(ATCCA**9**TTATGA)	**21**				
5′-d(TAGGT**A**AATACT)	**24**	8	32	−18	−6.6
3′-d(ATCCA**9**TTATGA)	**21**				
5′-d(TAGGT**G**AATACT)[43]	**22**	7	30	−20	−6.4
3′-d(ATCCA**G**TTATGA)	**19**				
5′-d(TAGGT**T**AATACT)[43]	**23**	7	36	−14	−7.8
3′-d(ATCCA**G**TTATGA)	**19**				
5′-d(TAGGT**A**AATACT)[43]	**24**	7	35	−15	−7.3
3′-d(ATCCA**G**TTATGA)	**19**				

[a] Measured at 260 nm in 1.0 M NaCl, 0.1 M $MgCl_2$, 60 mM Na-cacodylate buffer, with 5 μM + 5 μM single-strand concentration. [b] ΔT_m was calculated as $T_m^{basemismatch} - T_m^{basematch}$. [c] ΔG values are given in kcal mol^{-1} and have a standard error of less than 10%.

3. Photophysical properties

In contrast to 2′-deoxyguanosine, 8-aza-2′-deoxyguanosine (**9**) shows noticeable fluorescence at neutral pH and a strong fluorescence under alkaline condition (Fig. 2). This property has already been reported for 8-azaguanosine[20,34] and related 8-azapurine

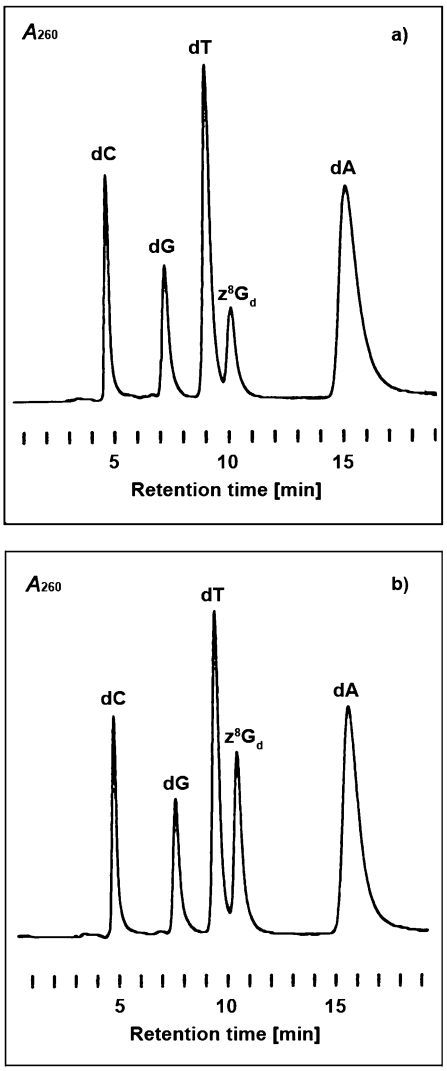

Fig. 1 Reversed-phase HPLC profiles (column RP-18) obtained after the enzymatic digest of a) oligonucleotide **21** containing **9** and b) oligonucleotide **21** after addition of **9**. The hydrolysis was performed with snake-venom phosphodiesterase and alkaline phosphatase in 0.1 M Tris·HCl buffer (pH 8.3) at 37 °C. Eluent: 0.1 M $(Et_3NH)OAc$ (pH 7.0)/MeCN, 95:5 with a flow rate of 0.8 $cm^3\ min^{-1}$.

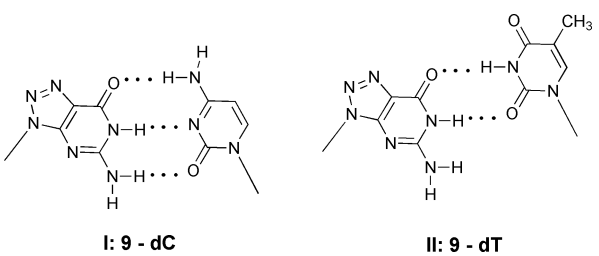

Scheme 4 Base pairs of nucleoside **9** with dC or dT.

nucleosides.[44] The pH-dependent change of emission was used to determine the pK_a value of deprotonation of nucleoside **9** (Scheme 5), which (as shown in Fig. 2b) is 8.4. An almost identical pK_a value (8.3) is obtained UV spectrophotometrically (Fig. 3b). From these data it is apparent that nucleoside **9** is more acidic than 2′-deoxyguanosine (pK_a = 9.3),[45] which is caused

Table 3 T_m values of oligonucleotide duplexes containing 8-aza-2′-deoxyguanosine **9** at pH 8.4 and 9.3.[a]

Duplex		pH 8.4		pH 9.3	
		T_m [°C]	ΔT_m [°C]	T_m [°C]	ΔT_m [°C]
5′-d(TAGGTCAATACT)	**18**	49		48	
3′-d(ATCCAGTTATGA)	**19**				
5′-d(TAGGTCAATACT)	**18**	49		46	
3′-d(ATCCA**9**TTATGA)	**21**				
5′-d(TAGGT**G**AATACT)	**22**	29	−20	29	−17
3′-d(ATCCA**9**TTATGA)	**21**				
5′-d(TAGGT**T**AATACT)	**23**	34	−15	31	−15
3′-d(ATCCA**9**TTATGA)	**21**				
5′-d(TAGGT**A**AATACT)	**24**	31	−18	30	−16
3′-d(ATCCA**9**TTATGA)	**21**				

[a] Measured in 1.0 M NaCl, 60 mM Na-cacodylate buffer, with 5 μM + 5 μM single-strand concentration.

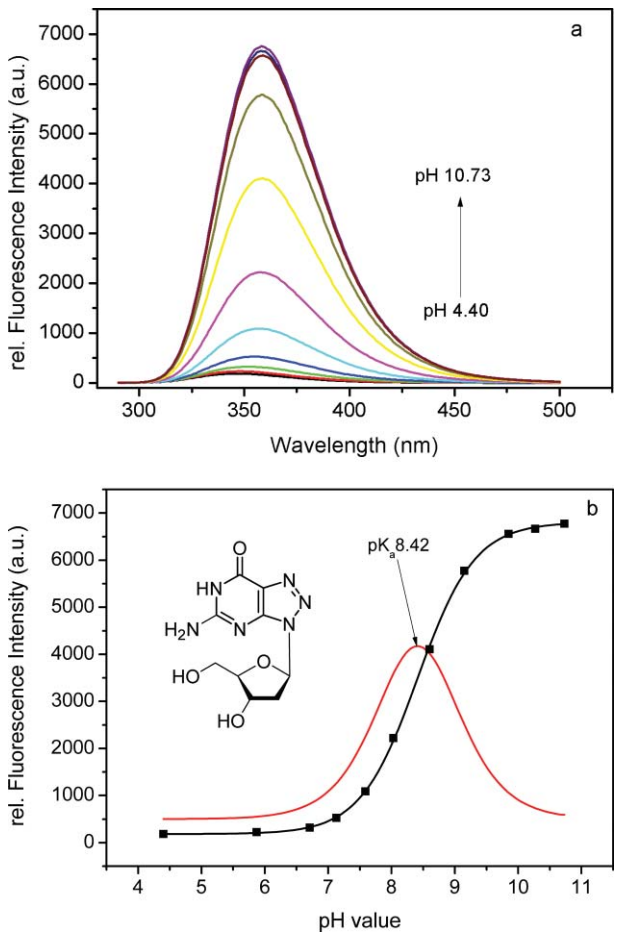

Fig. 2 (a) pH-dependent fluorescence spectra of 8-aza-2′-deoxyguanosine (**9**) measured in 0.1 M sodium phosphate buffer. For excitation and emission wavelengths see the ESI.† (b) Graph of fluorescence emission against pH value (sigmoidal curve) and its first derivative using data from (a).

by the electronegative nitrogen in position-8. It is also obvious that a strong bathochomic UV shift occurs (24 nm) when the nucleobase is deprotonated (pH 4.4: λ_{max} = 254 nm; pH 10.7: λ_{max} = 278 nm; Fig. 3a). See the ESI† for more details. A wavelength shift is also seen in the fluorescence spectra. The excitation

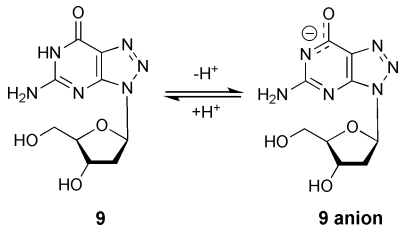

Scheme 5 The neutral and anionic forms of nucleoside **9**.

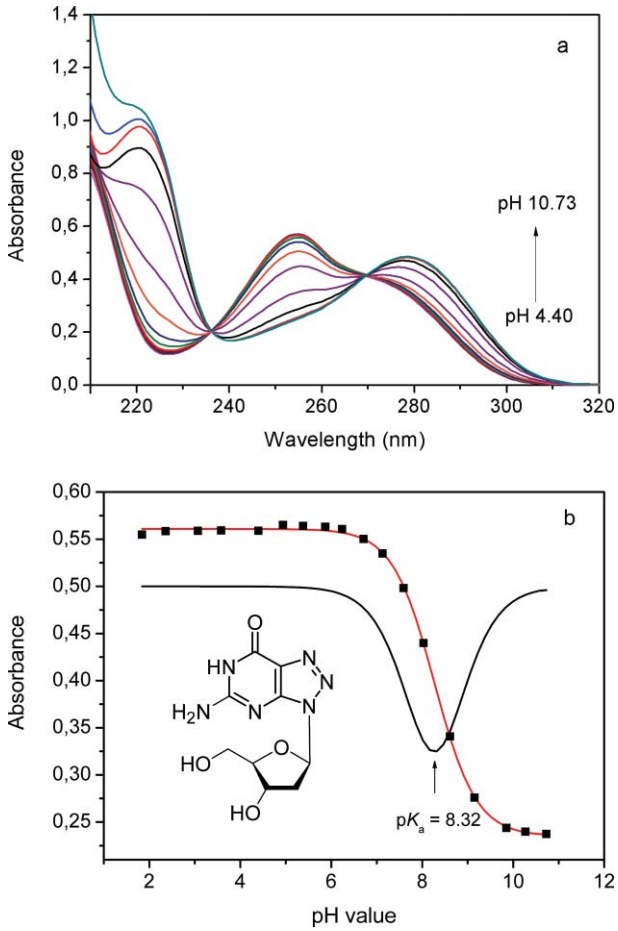

Fig. 3 (a) UV spectroscopic change of 8-aza-2′-deoxyguanosine (**9**) at various pH values measured in 0.1 M sodium phosphate buffer and (b) graph of absorbance *vs.* pH-value and its first derivative using data from (a).

wavelength shifts from 254 nm (pH 4.4) to 278 nm (pH 10.7), the emission wavelength from 345 nm (pH 4.4) to 359 nm (pH 10.7), and the fluorescence intensity increases from 170 to 6800.

Nucleosides have different pK_a values as monomeric compounds compared to when they are constituents of oligonucleotides. Changes are also seen between single strands and duplexes. While the pK_a-values of monomeric nucleosides can be easily determined UV-spectrophotometrically, the method has its limitation when the nucleoside is constituent of an oligonucleotide. This results from the similar shape and the overlap of the UV spectra of nucleobases within an oligonucleotide chain. The problem is circumvented by NMR-measurements, where a particular base moiety can be identified.[46] As canonical DNA and RNA bases are non-fluorescent, fluorescence techniques can be only employed with the help of fluorescent nucleobase analogues.

Fig. 4 shows the fluorescence changes of compound **9** as a function of the pH value for the free nucleoside monomer **9** (a) or as a constituent of the single-stranded oligonucleotide 3′-d(ATCCA**9**TTATGA) (**21**) (b). It is apparent that the fluorescence increases with increasing pH (nucleoside anion formation; Fig. 4a), and that the fluorescence is quenched by a factor of more than 10 when it is part of the oligonucleotide chain (Fig. 4b). A fluorescence decrease is usually observed for fluorescent nucleosides incorporated in oligonucleotides. Nevertheless, the decrease found for **9** is significantly less pronounced than for other fluorescent nucleoside analogues such as 2-aminopurine nucleoside **2b**.[13]

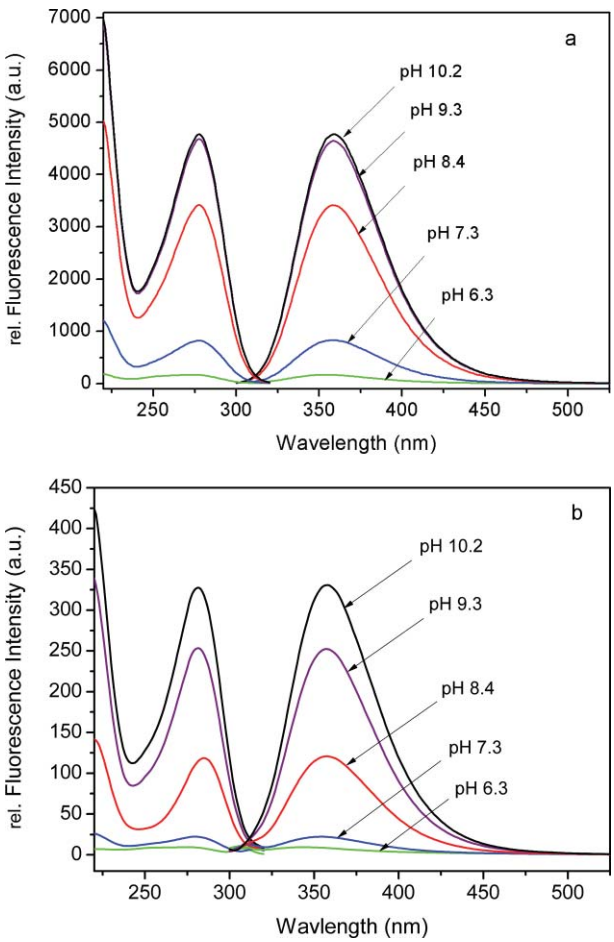

Fig. 4 Fluorescence excitation and emission spectra of (a) 8-aza-2′-deoxyguanosine (**9**) (5 μM concentration) and (b) **9** as constituent of the single-stranded oligonucleotide **21** (5 μM single-strand concentration) at different pH values. The spectra were measured in 1.0 M NaCl, 60 mM Na-cacodyate buffer.

Next, the pH-dependent fluorescence of the free nucleoside **9** and **9** as a constituent of the single-stranded (ss) oligonucleotide 3′-d(ATCCA**9**TTATGA) (**21**) and of the duplex (ds) 5′-d(TAGGTCAATACT) (**18**) · 3′-d(ATCCA**9**TTATGA) (**21**) was measured. From Fig. 5 it is obvious that the pK_a value of the nucleoside increases in alkaline medium when **9** is part of an oligonucleotide; the pK_a changes from 8.4 (nucleoside **9**) to

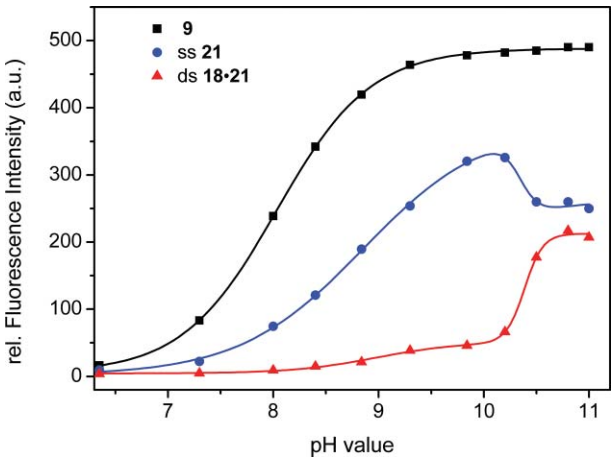

Fig. 5 Relative fluorescence intensity changes of 8-aza-2′-deoxyguanosine (**9**), ss oligonucleotide **21** containing **9** as constituent and within the duplex **18**·**21**. Measurements were performed in 1.0 M NaCl, 60 mM Na-cacodyate buffer (5 μM concentration for each ss oligonucleotide and 0.5 μM concentration for the free nucleoside **9**). Excitation wavelength = 277 nm; emission at 360 nm. The pK_a value is 8.4 for nucleoside **9**; 8.8 and 10.3 for **9** in ss **21**; 9.1 and 10.4 for the duplex **18**·**21**.

8.8 (ss-oligonucleotide **21**); negative phosphodiester charges protect the base of **9** from deprotonation. At higher pH-values, the fluorescence of the ss-oligonucleotide **21** decreases, resulting in an inflection point at pH 10.3. We suggest that the first pK_a change is due to the deprotonation of the nucleoside **9** residue without deprotonation of the other bases within the oligonucleotide, while the second one results from complete deprotonation to form dG and dT anions. Negative charges are now present on the nucleobases of dG and dT and the phosphodiester residues, a phenomenon which apparently has a negative effect on the fluorescence of **9** (Scheme 6A).

Deprotonation is more difficult when the lactam proton of **9** is not free and part of the **9**·dC base pair. According to Fig. 4b, which is also shown in more detail in the ESI,† two pK_a-values were detected between pH 6.3–11.0 for the duplex **18**·**21**. The first pK_a value results from the deprotonation of the **9**·dC base pair within the duplex. This can cause a bulged loop duplex structure as shown in Scheme 6. This pK_a value (9.1) is higher than that of the single-stranded oligonucleotide **21** (pK_a = 8.8) as all other base pairs are not opened; the fluorescence increase is small as all bases are still stacked. A further pH increase leads to duplex "melting" with the formation of two single-strands (**18** and **21**; Scheme 6). Now, the nucleoside **9** residue is released from the duplex stack and the Watson–Crick face becomes freely accessible to water molecules. As a consequence, a hyperchromic fluorescence change occurs, with the inflection point being similar to that observed for the single-stranded **21** during complete deprotonation (Scheme 6).

4. Mismatch discrimination, fluorescence quenching and duplex structure

The fluorescence measurements of **9** do not just allow measurements of pK_a values within oligonucleotide single-strands and duplexes but also offer the opportunity to use such fluorescent molecules for SNP (single-nucleoside polymorphism) detection.[47,48] Thermodynamic differences of duplex melting

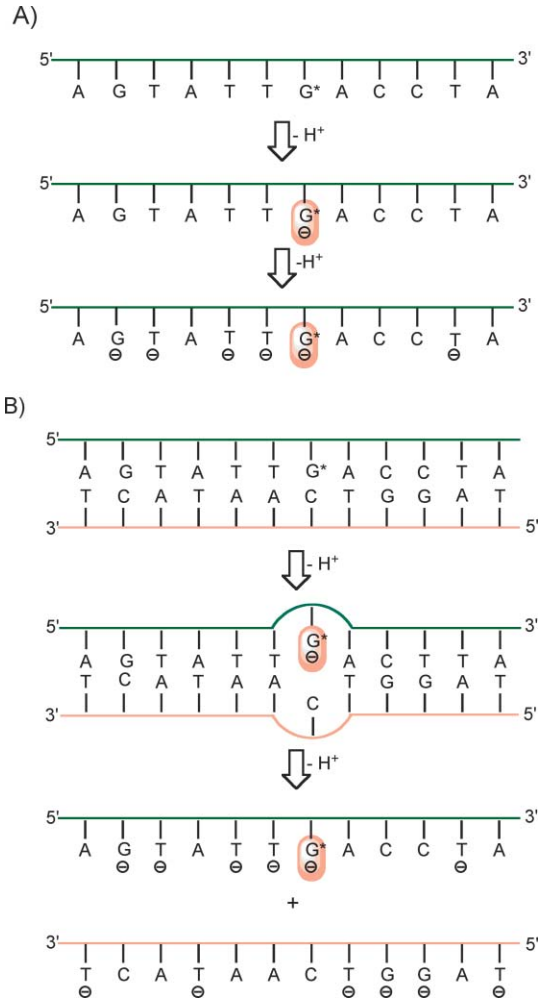

Scheme 6 Stepwise deprotonation of (A) the ss-oligonucleotide **21** and (B) the oligonucleotide duplex **18**·**21** according to Fig. 5. A = adenine, G = guanine, C = cytosine, T = thymine, G* = 8-azaguanine.

(ΔT_m values) are often too small in DNA to distinguish between matches and mismatches. Consequently, in DNA probes these changes cannot be measured accurately. Fluorescence measurements are more sensitive, as fluorescent intercalating dyes can be used to detect mismatch formation.[49] A more direct approach uses dyes directly attached to a nucleoside residue of an oligonucleotide.[50–52] However, dye stacking can obscure data. Thus, modified nucleosides with "built-in" fluorescence are valuable for such protocols.

As it is possible to incorporate compound **9** efficiently into primer and probes by solid-phase oligonucleotide synthesis, nucleobase matches and mismatches formed by the modified nucleoside **9** are expected to be detected by fluorescence measurements. For mismatch discrimination by fluorescence detection, a solution of the ss oligonucleotide **21** (1 cm^3) was prepared at a defined concentration and a fixed pH-value; then 2 μl of a stock solution of the individual oligonucleotide (**18**, **22**, **23** or **24**) forming a particular mismatch was added, resulting in a final single-strand concentration of 5 μM for each strand. Fluorescence spectra of oligonucleotide duplexes were measured in which the four canonical nucleosides were placed opposite to the modification site (5′-d(TAGGT**X**AATACT) · 3′-d(ATCCA**9**TTATGA), X = dA,

dG, dT, dC). The fluorescence of single-strand **21** was measured for comparison. Measurements were performed at two pH values (8.4 and 9.3). The fluorescence emission curves are shown in Fig. 6a,b and in the corresponding bar charts (Fig. 6c,d). The fluorescence quenching is 6–7 fold in the dC·**9** pair compared to the ss-oligonucleotide **21**; in the other three cases quenching is about 2-fold (Fig. 6c, d). The fluorescence decreases in the following order of base pairs: dC·**9** ≫ dT·**9** > dA·**9** > dG·**9** as a result of the decreasing duplex stability. The same order is found from the T_m measurements shown in Table 3. The T_m values at pH 8.4 decrease from the dC·**9** pair (49 °C) *via* the dT·**9** pair to the mismatches dA·**9** and dG·**9**, which are 15 °C, 18 °C and 20 °C lower than that of the dC·**9** duplex.

To get a more detailed view on the structure of duplexes incorporating matches and mismatches, molecular models were constructed using the program Hyperchem 8.0 (Hypercube Inc., Gainesville, FL, USA, 2001). The energy was minimized by AMBER calculations. From Fig. 7 it is apparent that replacing dG with nucleoside **9** does not perturb the structure of the unmodified duplex **18**·**19** (Fig. 7A,B), and also that the dT·**9** pair is well accommodated in duplex oligonucleotides **23**·**21** (Fig. 7F). The positioning of **9** opposite to the canonical purine nucleoside as in dA·**9** or dG·**9** disturbs the helix structure (Fig. 7E,D). In all three mismatch situations the fluorescence is significantly increased over the duplex **18**·**21**.

Conclusion

The anion of 8-aza-2′-deoxyguanosine (**9**) is fluorescent. Its glycosylic bond is more stable than that of the parent purine nucleoside,[53] and it prevents dG-quartet formation.[26] It is an ideal shape mimic of dG for fluorescence studies on single-stranded and duplex DNA. Its pK_a value (8.4) is lower than that of dG (9.3) and similar to the ribonucleoside.[20,21] The pK_a value is shifted toward the alkaline medium from single-stranded oligonucleotides (pK_a 8.8) to duplex DNA (pK_a 9.1). These properties can be used to detect changes in the microenvironment of a base pair. It offers a way to detect mismatches by nucleobase anion fluorescence sensing. For nucleoside **9**, the stability of matches and mismatches decreases in the order dC·**9** ≫ dT·**9** > dA·**9** > dG·**9** as determined from UV-melting profiles. The same order is observed from fluorescence measurements. As a result, the stability of a base pair is displayed by the fluorescence intensity measured under slightly alkaline conditions, reflecting the degree of deprotonation of the nucleoside **9**.

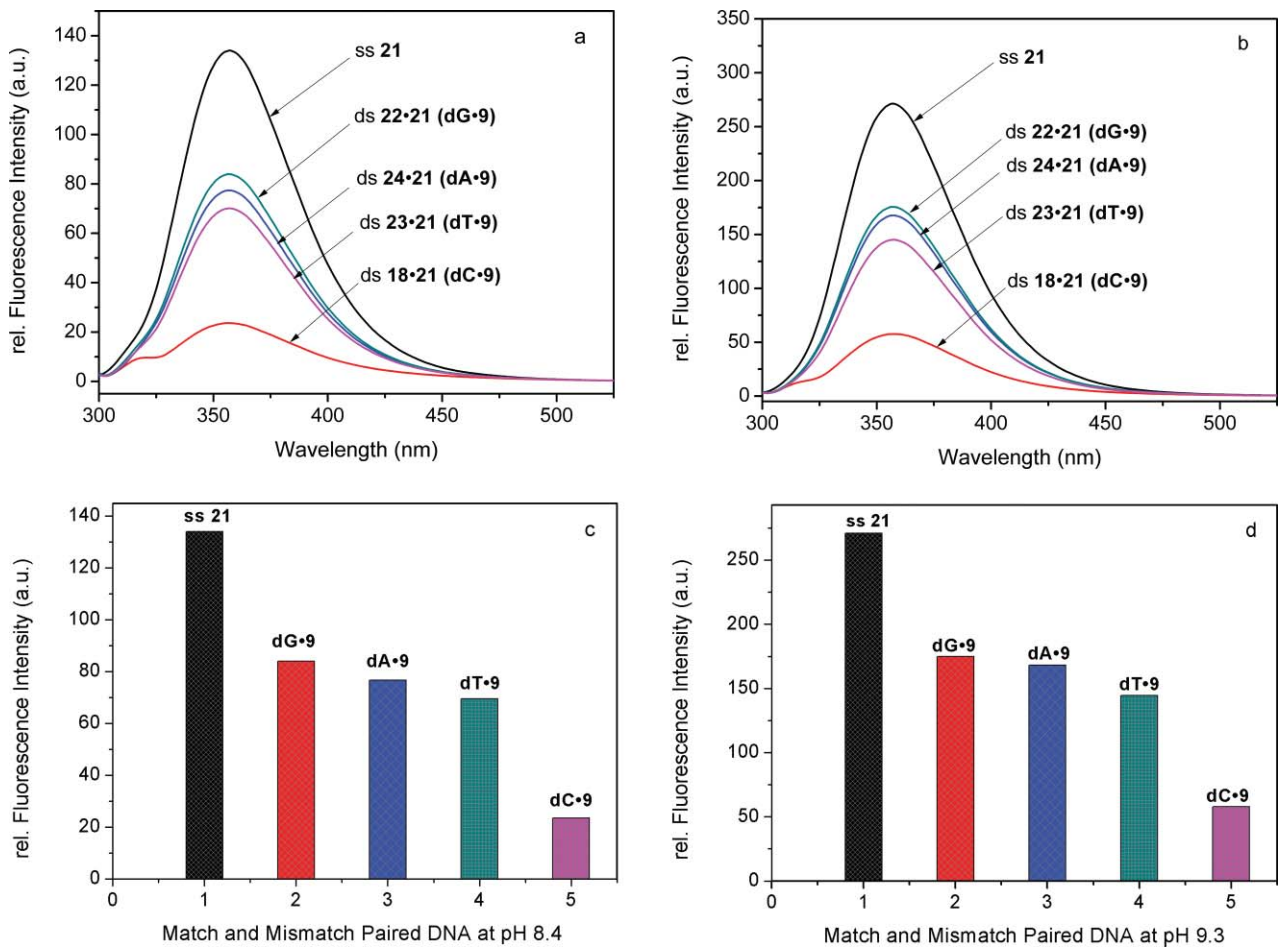

Fig. 6 Fluorescence emission spectra of 8-aza-2′-deoxyguanosine (**9**) as constituent of the single-stranded oligonucleotide **21** and in paired duplexes (**18**·**21**, **22**·**21**, **23**·**21**, **24**·**21**) at (a) pH 8.4 and (b) pH 9.3. Bar charts for (c) pH 8.4 and (d) pH 9.3. The curves were measured in 1.0 M NaCl and 60 mM Na-cacodyate buffer. Single-strand concentration: 5 μM each.

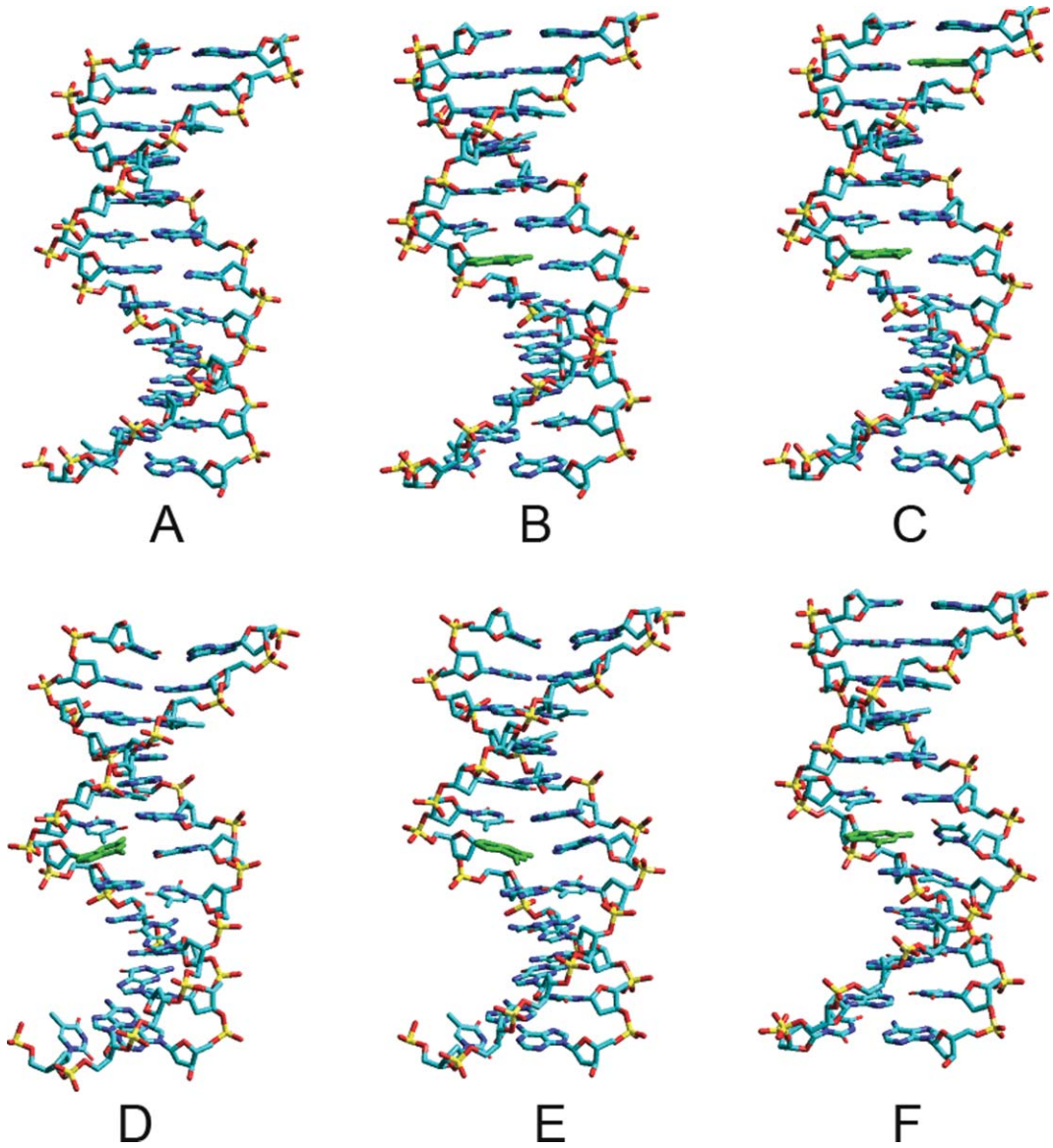

Fig. 7 Molecular models of (A) duplex **18**·**19** (dC·dG), (B) duplex **18**·**21** (dC·**9**), (C) duplex **18**·**20** (dC·**9**) (two nucleoside **9** modifications), (D) duplex **22**·**21** (dG·**9**), (E) duplex **24**·**21** (dA·**9**), (F) duplex **23**·**21** (dT·**9**). The models were calculated using the program Hyperchem 8.0; the energy was minimized by AMBER calculations.

Experimental

General

All chemicals were purchased from Acros, Aldrich, Sigma, or Fluka (Sigma-Aldrich Chemie GmbH, Deisenhofen, Germany). Solvents were of laboratory grade. Thin-layer chromatography (TLC) was performed on TLC aluminium sheets covered with silica gel 60 F254 (0.2 mm, VWR International, Germany). Column flash chromatography (FC): silica gel 60 (VWR International, Darmstadt, Germany) at 0.4 bar; UV-spectra were recorded on a U-3000 spectrophotometer (Hitachi, Japan), $\lambda_{max.}$ in nm, ε in $dm^3\ mol^{-1}\ cm^{-1}$. NMR spectra: DPX 300 spectrometers (Bruker, Germany) at 300 MHz for ^1H and 75 MHz for ^{13}C. The *J* values are given in Hz; δ values in ppm relative to Me_4Si as internal standard, or 85% H_3PO_4 for ^{31}P. Elemental analyses were performed by the Mikroanalytisches Laboratorium Beller, Göttingen, Germany. Reversed-phase HPLC was carried out on a 4 × 250 mm RP-18 (10 μm) LiChrospher 100 column (VWR International) with a Merck-Hitachi HPLC pump (Model L-6250) connected with a variable wavelength monitor (model 655-A), a controller (model L-500) and an integrator (model D-2500). MALDI-TOF mass spectra were recorded on a Applied Biosystems Voyager DE PRO spectrometer (Bruker, Leipzig, Germany) in a linear mode with 3-hydroxypicolinic acid (3-HPA) as a matrix. The melting temperature curves were measured with a Cary-100 Bio UV-VIS spectrophotometer (Varian, Australia) equipped with a Cary thermoelectrical controller. The temperature was measured continuously in the reference cell with a Pt-100 resistor with a heating rate of 1 °C min^{-1}.

Fluorescence measurements

The fluorescence measurements were performed in distilled water at 20 °C. Fluorescence spectra were recorded in the wavelength range between 300 to 600 nm using the fluorescence spectrophotometer F-2500 (Hitachi, Tokyo, Japan). In order to avoid inner filter effects, the sample was not allowed to exceed 0.1 at the excitation wavelength using standard quartz cuvettes with a path length of 1 cm.

pK_a determination by fluorescence. Nucleoside **9** was dissolved in 0.1 M sodium phosphate buffer, pH 4.4. NaOH solution (4 M) was used to adjust the pH value of the buffer. At defined pH values, the fluorescence of nucleoside **9** was measured. At each pH value an excitation spectrum was measured and the maximum wavelength obtained from this spectrum was used to record the emission spectrum. For excitation and emission wavelengths see Table S1.†

Fluorescence measurements of nucleoside 9, ss- and ds-oligonucleotides. An aqueous solution (100 cm^3) containing 1.0 M NaCl, 60 mM Na-cacodylate buffer was adjusted with 4 M aq. NaOH to a defined pH value. To 1 cm^3 of each solution, a defined amount (0.002 to 0.005 cm^3) of a stock solution containing either the nucleoside **9** or the ss oligonucleotide **21** were added. Excitation and emission spectra were recorded at different pH values (Fig. 4).

For hybridization, to the solutions mentioned above, 0.002 cm^3 of a stock solution of the individual oligonucleotide (**18**, **22**, **23** or **24**) was introduced, resulting in a final single-strand concentration of 5 μM for each strand. Fluorescence spectra were measured; results are shown in Figs. 5 and 6.

Synthesis and characterization of oligonucleotides

The oligonucleotide synthesis was performed on an ABI 392-08 synthesizer (Applied Biosystem, Weiterstadt, Germany) on a 1 μmol scale (trityl-on mode) employing the standard phosphoramidites and the modified building block **11** and following the synthesis protocol for 3′-cyanoethyl phosphoramidites (User's Manual of the DNA Synthesizer, Applied Biosystems, Weiterstadt, Germany).[54] The average coupling yield was always higher than 95%. After cleavage from the solid-support, the oligonucleotides were deprotected in 25% aq. NH_3 for 16 h at 60 °C. The DMT-containing oligonucleotides were purified by reversed-phase HPLC (RP-18) with the following solvent gradient system [A: 0.1 M $(Et_3NH)OAc$ (pH 7.0)/MeCN 95:5; B: MeCN; gradient I: 0–3 min 10–15% B in A, 3–15 min 15–50% B in A, 15–20 min 50–10% B in A, flow rate 0.8 cm^3 min^{-1}]. Then, the mixture was evaporated to dryness, and the residue was treated with 2.5% $Cl_2CHCOOH/CH_2Cl_2$ for 3 min at 0 °C to remove the 4,4′-dimethoxytrityl residues. The detritylated oligomers were purified by reversed-phase HPLC with gradient II: 0–25 min 0–20% B in A, 25–30 min 20% B in A, 30–35 min 20–0% B in A, flow rate 0.8 cm^3 min^{-1}. The oligomers were desalted on a short column (RP-18, silica gel) using H_2O for elution of the salt, while the oligomers were eluted with $MeOH/H_2O$ (3:2). The oligonucleotides were lyophilized on a Speed Vac evaporator to yield colourless solids which were stored frozen at –24 °C. The enzymatic hydrolysis of the oligonucleotides was performed as described[41] with snake-venom phosphodiesterase (EC 3.1.15.1, *Crotallus adamanteus*) and alkaline phosphatase (EC 3.1.3.1, *Escherichia coli* from Roche Diagnostics GmbH, Germany) in 0.1 M Tris·HCl buffer (pH 8.3) at 37°C, which was carried out on reversed-phase HPLC (RP-18; 260 nm; eluent: 0–20 min A, A = 0.1 M $(Et_3NH)OAc$ (pH 7.0)/MeCN 95:5, flow rate: 0.8 cm^3 min^{-1}) showing the peaks of the modified **9** and unmodified nucleosides. Quantification of the constituents was made on the basis of the peak areas, which were divided by the extinction coefficients of the nucleosides (ε_{260}): dT 8800, dC 7300, dA 15400, dG 11700, z^8G_d (**9**) 12700.

Table 4 Molecular masses determined from MALDI-TOF mass spectra

Oligonucleotides		$[M-1]^-$ (calcd)	$[M-1]^-$ (found)
3′-d(ATCCA**9**TTAT**9**A)	**20**	3645.7	3645.67
3′-d(ATCCA**9**TTATGA)	**21**	3645.7	3645.05

The molecular masses of the oligonucleotides **20** and **21** were determined by MALDI-TOF mass spectrometry in the linear negative mode. The detected masses were identical with the calculated values (Table 4).

5-Amino-3-[2-deoxy-3,5-di-*O*-(*p*-toluoyl)-β-D-*erythro*-pentofuranosyl]-3,6-dihydro-7*H*-1,2,3-triazolo[4,5-*d*]pyrimidin-7-one (15). A suspension of 8-azaguanine (**12**, 3.0 g, 19.7 mmol) in hexamethyl disilazane (60 cm^3) was refluxed in the presence of a catalytic amount of $(NH_4)_2SO_4$ for 4 h until a clear solution was obtained. The excess of HMDS was removed *in vacuo* and 2-deoxy-3,5-di-*O*-*p*-toluoyl-α-D-*erythro*-pentofuranosyl chloride[55,56] (**13**) (7.7 g, 19.8 mmol) in a minimal amount of CH_2Cl_2, was added to give a solution. The CH_2Cl_2 was removed under reduced pressure. The residue formed was heated under aspirator vacuum to 130 °C and the solution formed was stirred at this temperature for 1 h. The reaction mixture was cooled and 50 cm^3 ethyl acetate was added followed by 20% aqueous EtOH (20 cm^3). The mixture was stirred at room temperature for 2 h. The solvent was removed by evaporation and the residue (HPLC shows a mixture of **14** and **15** with a ratio of 1:1) was dissolved in hot ethyl acetate (3 dm^3). After filtration through a Celite 45 pad, the filtrate was removed by evaporation to a volume of about 100 cm^3. This solution was kept at room temperature overnight and colourless crystals were formed, which were collected by filtration. This product was recrystallized from ethyl acetate (100 cm^3), again giving compound **15** (3.0 g, yield 30%) with less than 2% α-D anomer (determined by HPLC; t_R (**14**) = 10.2 and t_R (**15**) = 12.5 (RP-18 column); eluent: 50% A and 50% B with a flow rate of 0.8 cm^3 min^{-1}). TLC (silica gel, CH_2Cl_2/CH_3OH 20:1): R_f 0.21. UV (MeOH): 242 (38500). δ_H (300 MHz, [d_6]DMSO, Me_4Si) 2.35–2.38 (6 H, d, *J* 8.1, 2 × CH_3), 2.79–2.86 (1 H, m, 2′-H_α), 3.34–3.37 (1 H, m, 2′-H_β), 4.39–4.59 (3 H, m, 2 × 5′-H, 4′-H), 5.84 (1 H, s, 3′-H), 6.50 (1 H, 't', *J* 6.1, 1′-H), 7.01 (2 H, br s, NH_2), 7.19–7.94 (8 H, m, arom. H), 11.07 (1 H, br s, NH).

5-Amino-3-[2-deoxy-β-D-*erythro*-pentofuranosyl]-3,6-dihydro-7*H*-1,2,3-triazolo[4,5-*d*] pyrimidin-7-one (9). A solution of compound **15** (1.63 g, 3.26 mmol) in 50 cm^3 methanolic ammonia was stirred at 60 °C in an autoclave overnight. The solvent was evaporated and the residue was triturated with CH_2Cl_2 (4 × 10 cm^3). The crude product was dissolved in 25% aqueous ethanol with heating, and active charcoal was added. After hot filtration,

the filtrate was evaporated until a thick suspension was formed. The solvent was removed by filtration and the solid was dried, affording a colorless solid of **9** (510 mg, 59%). TLC (silica gel, CH_2Cl_2/CH_3OH 5:1): R_f 0.24. UV (MeOH): 257 (13400). δ_H (300 MHz, [d_6]DMSO, Me_4Si) 2.30–2.34 (1 H, m, 2′-H_α), 2.83–2.92 (1 H, m, 2′-H_β), 3.46–3.50 (2 H, m, 2 × 5′-H), 3.80–3.81 (1H, m, 4′-H), 4.43 (1 H, s, 3′-H), 4.74 (1 H, s, 5′-OH), 5.31 (1 H, s, 3′-OH), 6.26 (1 H, 't', *J* 6.1, 1′-H), 6.95 (1 H, br s, NH_2), 11.05 (1 H, br s, NH). For elemental analysis and melting point see ref. 27.

3-(2-Deoxy-β-D-*erythro*-pentofuranosyl)-5-[(di-*n*-butylamino)-methylidene]amino-3,6-dihydro-7*H*-1,2,3-triazolo[4,5-*d*]pyrimidin-7-one (16). A suspension of compound **9** (500 mg, 1.86 mmol) in methanol (30 cm^3) was stirred with *N*,*N*-dibutylformamide dimethyl acetal (1.5 cm^3, 12.5 mmol) at room temperature overnight. The solvent was evaporated and applied to FC (silica gel, column 8 × 5 cm). Elution with CH_2Cl_2/CH_3OH (50:1) yielded **16** as a colorless foam (640 mg, 84%). TLC (silica gel, CH_2Cl_2/CH_3OH 10:1): R_f 0.40. UV (MeOH): 246 (13500), 303 (26200). δ_H (300 MHz, [d_6]DMSO, Me_4Si) 0.88–0.93 (6 H, m, 2 × CH_3), 1.24–1.33 (4 H, m, 2 × CH_2), 1.53–1.59 (4 H, m, 2 × CH_2), 2.33–2.39 (1 H, m, 2′-H_α), 2.87–2.96 (1 H, m, 2′-H_β), 3.39–3.57 (6 H, m, 2 × 5′-H, 2 × NCH_2), 3.87 (1 H, t, *J* 4.5, 4′-H), 4.50 (1 H, t, *J* 4.5, 3′-H), 4.78 (1 H, t, *J* 5.7, 5′-OH), 5.37 (1 H, d, *J* 4.2, 3′-OH), 6.45 (1 H, 't', *J* 6.3, 1′-H), 8.67 (1 H, s, N=CH), 11.67 (1 H, s, NH). Anal. Calcd for $C_{18}H_{29}N_7O_4$ (407.47): C, 53.06; H, 7.17; N, 24.06. Found: C, 53.20; H, 7.28; N, 23.90.

3-[2-Deoxy-5-*O*-(4,4′-dimethoxytriphenylmethyl)-β-D-*erythro*-pentofuranosyl]-5-[(di-*n*-butylamino)methylidene]amino-3,6-dihydro-7*H*-1,2,3-triazolo[4,5-*d*]pyrimidin-7-one (17). Compound **16** (204 mg, 0.50 mmol) was coevaporated with anhydrous pyridine 3 times and dissolved in anhydrous pyridine (5 cm^3). 4,4′-Dimethoxytriphenylmethyl chloride (202 mg, 0.60 mmol) was added. The mixture was stirred at room temperature. After 2 h the solvent was evaporated and applied to FC (silica gel, column 8 × 5 cm). Elution with CH_2Cl_2/CH_3OH (100:1 → 50:1) yielded the compound **17** as a colorless foam (267 mg, 75%). TLC (silica gel, CH_2Cl_2/CH_3OH 20:1): R_f 0.30. UV (MeOH): 235 (31500), 304 (28200). δ_H (300 MHz, [d_6]DMSO, Me_4Si) 0.85–0.93 (6 H, m, 2 × CH_3), 1.20–1.33 (4 H, m, 2 × CH_2), 1.51–1.60 (4 H, m, 2 × CH_2), 2.49–2.51(1 H, m, 2′-H_α), 2.85–2.94 (1 H, m, 2′-H_β), 3.01–3.10 (2 H, m, NCH_2), 3.35–3.50 (4 H, m, 2 × 5′-H, NCH_2), 3.70 (3 H, s, OCH_3), 3.71 (3 H, s, OCH_3), 3.95–4.00 (1 H, m, 4′-H), 4.55–4.63 (1 H, m, 3′-H), 5.42 (1 H, d, *J* 4.8, 3′-OH), 6.50 (1 H, 't', *J* 3.6, 1′-H), 6.71–7.30 (13 H, m, arom. H), 8.67 (1 H, s, N=CH), 11.71 (1 H, s, NH). Anal. Calcd for $C_{39}H_{47}N_7O_6$ (709.83): C, 65.99; H, 6.67; N, 13.81. Found: C, 65.89; H, 6.66; N, 14.07.

3-{2-Deoxy-5-*O*-(4,4′-dimethoxytriphenylmethyl)-3-*O*-[(2-cyanoethyl)-*N*,*N*-diisopropyl-phosphoramidite]-β-D-*erythro*-pentofuranosyl}-5-[(di-*n*-butylaminoamino)methylidene]amino-3,6-dihydro-7*H*-1,2,3-triazolo[4,5-*d*]pyrimidin-7-one (11). To a solution of compound **17** (560 mg, 0.79 mmol) in CH_2Cl_2 (10 cm^3), $(iPr)_2NEt$ (0.3 cm^3, 1.9 mmol) and 2-cyanoethyl diisopropylphosphoramido chloridite (0.5 cm^3, 2.2 mmol) were added. The mixture was stirred at room temperature for 20 min and diluted with CH_2Cl_2 (50 cm^3). The mixture was washed with 5% aqueous $NaHCO_3$ (50 cm^3) and dried with Na_2SO_4. After filtration, the filtrate was evaporated. The residue was applied to FC (silica gel, column 10 × 3 cm, eluted with CH_2Cl_2/acetone 95:5) yielding **11** as a colorless foam (620 mg, 86%). TLC (CH_2Cl_2/acetone 9:1): R_f 0.4. δ_P (101 MHz, $CDCl_3$, H_3PO_4) 148.7.

Acknowledgements

We thank Mr. N. Q. Tran for the oligonucleotide synthesis and Dr. T. Koch from Roche Diagnostics, Penzberg, for the measurement of the MALDI spectra. We appreciate critical reading of the manuscript by Dr. P. Leonard, Dr. S. Budow and Mr. S. Pujari. Financial support by Roche Diagnostics GmbH, Penzberg, and ChemBiotech, Münster, Germany, is gratefully acknowledged.

References

1 P. R. Callis, *Annu. Rev. Phys. Chem.*, 1983, **34**, 329–357.
2 D. C. Ward, E. Reich and L. Stryer, *J. Biol. Chem.*, 1969, **244**, 1228–1237.
3 S. R. Kirk, N. W. Luedtke and Y. Tor, *Bioorg. Med. Chem.*, 2001, **9**, 2295–2301.
4 A. Holy, *Collect. Czech. Chem. Commun.*, 1979, **44**, 2846–2853.
5 F. Seela, Y. Chen, U. Bindig and Z. Kazimierczuk, *Helv. Chim. Acta*, 1994, **77**, 194–202.
6 F. Seela, H. Steker, H. Driller and U. Bindig, *Liebigs Ann. Chem.*, 1987, 15–19.
7 F. Seela and H. Steker, *Liebigs Ann. Chem.*, 1984, 1719–1730.
8 J. N. Wilson and E. T. Kool, *Org. Biomol. Chem.*, 2006, **4**, 4265–4274.
9 J. A. Secrist III, J. R. Barrio, N. J. Leonard and G. Weber, *Biochemistry*, 1972, **11**, 3499–3506.
10 Y. Inoue, T. Kuramochi and K. Imakubo, *Chem. Lett.*, 1981, 1161–1164.
11 J. Woo, R. B. Meyer Jr. and H. B. Gamper, *Nucleic Acids Res.*, 1996, **24**, 2470–2475.
12 D. A. Berry, K.-Y. Jung, D. S. Wise, A. D. Sercel, W. H. Pearson, H. Mackie, J. B. Randolph and R. L. Somers, *Tetrahedron Lett.*, 2004, **45**, 2457–2461.
13 F. Seela, E. Schweinberger, K. Xu, V. R. Sirivolu, H. Rosemeyer and E.-M. Becker, *Tetrahedron*, 2007, **63**, 3471–3482.
14 S. G. Srivatsan, H. Weizman and Y. Tor, *Org. Biomol. Chem.*, 2008, **6**, 1334–1338.
15 J. Ren and D. J. Goss, *Nucleic Acids Res.*, 1996, **24**, 3629–3634.
16 H. Kasai, M. Goto, K. Ikeda, M. Zama, Y. Mizuno, S. Takemura, S. Matsuura, T. Sugimoto and T. Goto, *Biochemistry*, 1976, **15**, 898–904.
17 P. D. Sattsangi, N. J. Leonard and C. R. Frihart, *J. Org. Chem.*, 1977, **42**, 3292–3296.
18 H. Bazin, X.-X. Zhou, C. Glemarec and J. Chattopadhyaya, *Tetrahedron Lett.*, 1987, **28**, 3275–3278.
19 F. Seela and W. Bussmann, *Tetrahedron*, 1985, **41**, 935–940.
20 J. Wierzchowski, B. Wielgus-Kutrowska and D. Shugar, *Biochim. Biophys. Acta*, 1996, **1290**, 9–17.
21 C. P. Da Costa, M. J. Fedor and L. G. Scott, *J. Am. Chem. Soc.*, 2007, **129**, 3426–3432.
22 J. Davoll, *J. Chem. Soc.*, 1958, 1593–1599.
23 G. R. Revankar and R. K. Robins, in *Chemistry of Nucleosides and Nucleotides*, ed. L. B. Townsend, Plenum Press, New York, London, 1991, vol. 2, ch. 4, pp. 297–318.
24 J. A. Montgomery, in *Handbuch der experimentellen Pharmakologie*, ed. O. Eichler, A. Farha, H. Herken and A. D. Welch, Springer, Heidelberg, 1974, vol. 28, p. 76.
25 R. Vince and M. Hua, *J. Med. Chem.*, 1990, **33**, 17–21.
26 F. Seela and S. Lampe, *Helv. Chim. Acta*, 1994, **77**, 1003–1017.
27 F. Seela and S. Lampe, *Helv. Chim. Acta*, 1993, **76**, 2388–2397.
28 F. Seela, A. M. Jawalekar and I. Münster, *Helv. Chim. Acta*, 2005, **88**, 751–765.
29 A. Albert, *Adv. Heterocycl. Chem.*, 1986, **39**, 117–180.
30 R. O. Roblin Jr., J. O. Lampen, J. P. English, Q. P. Cole and J. R. Vaughan Jr., *J. Am. Chem. Soc.*, 1945, **67**, 290–294.
31 G. W. Kidder, V. C. Dewey, R. E. Parks Jr. and G. L. Woodside, *Science*, 1949, **109**, 511–514.

32 G. W. Kidder, V. C. Dewey, R. E. Parks Jr. and G. L. Woodside, *Cancer. Res.*, 1951, **11**, 204–211.
33 R. E. F. Matthews and J. D. Smith, *Advan. Virus. Res.*, 1955, **3**, 49–148.
34 J. Wierzchowski, M. Ogiela, B. Iwańska and D. Shugar, *Anal. Chim. Acta*, 2002, **472**, 63–74.
35 J. Kára, J. Škoda and F. Šorm, *Collect. Czech. Chem. Commun.*, 1961, **26**, 1386–1392.
36 F. Seela and K. Mersmann, *Helv. Chim. Acta*, 1993, **76**, 2184–2193.
37 W. Hutzenlaub, R. L. Tolman and R. K. Robins, *J. Med. Chem.*, 1972, **15**, 879–883.
38 M. H. Caruthers, L. J. Mcbride, L. P. Bracco and J. W. Dubendorff, *Nucleosides Nucleotides*, 1985, **4**, 95–105.
39 L. G. Purnell and D. J. Hodgson, *Organic Magnetic Resonance*, 1977, **10**, 1–4.
40 F. Seela and W. Bussmann, *Nucleosides Nucleotides*, 1985, **4**, 391–394.
41 F. Seela and H. Driller, *Nucleic Acids Res.*, 1986, **14**, 2319–2332.
42 T. Brown, W. N. Hunter and G. A. Leonard, *Chem. Br.*, 1993, **29**, 484–487.
43 F. Seela and K. Xu, *Org. Biomol. Chem.*, 2008, **6**, 3552–3560.
44 G. Mędza, J. Wierzchowski, B. Kierdaszuk and D. Shugar, *Bioorg. Med. Chem.*, 2009, **17**, 2585–2591.
45 Y. Chiang and A. J. Kresge, *Org. Biomol. Chem.*, 2004, **2**, 1090–1092.
46 S. Acharya, J. Barman, P. Cheruku, S. Chatterjee, P. Acharya, J. Isaksson and J. Chattopadhyaya, *J. Am. Chem. Soc.*, 2004, **126**, 8674–8681.
47 S. Lohmann, L. Lehmann and K. Tabiti, *Biochemica*, 2000, 23–28.
48 A. Okamoto, K. Tanaka, T. Fukuta and I. Saito, *J. Am. Chem. Soc.*, 2003, **125**, 9296–9297.
49 L. Bethge, D. V. Jarikote and O. Seitz, *Bioorg. Med. Chem.*, 2008, **16**, 114–125.
50 A. Okamoto, K. Tainaka, Y. Ochi, K. Kanatani and I. Saito, *Mol. BioSyst.*, 2006, **2**, 122–127.
51 A. Okamoto, K. Kanatani and I. Saito, *J. Am. Chem. Soc.*, 2004, **126**, 4820–4827.
52 F. Seela, H. Xiong, P. Leonard and S. Budow, *Org. Biomol. Chem.*, 2009, **7**, 1374–1387.
53 R. Käppi, Z. Kazimierczuk, P. Järvinen, F. Seela and H. Lönnberg, *J. Chem. Soc. Perkin Trans. 2*, 1991, 595–600.
54 User's Manual of the DNA Synthesizer, Applied Biosystems, Weiterstadt, Germany.
55 M. Hoffer, *Chem. Ber.*, 1960, **93**, 2777–2781.
56 V. Rolland, M. Kotera and J. Lhomme, *Synth. Commun.*, 1997, **27**, 3505–3511.